Cleaning of Oil Fouling with Water Enabled by Zwitterionic Polyelectrolyte Coatings: Overcoming the Imperative Challenge of Oil–Water Separation Membranes

Ke He,[†,‡] Haoran Duan,[†] George Y. Chen,[§] Xiaokong Liu,[*,†] Wensheng Yang,[‡] and Dayang Wang[†]

[†]Ian Wark Research Institute, University of South Australia, Mawson Lakes, South Australia 5095, Australia, [‡]State Key Laboratory of Supramolecular Structure and Materials, College of Chemistry, Jilin University, Changchun 130012, PR China, and [§]Laser Physics and Photonic Devices Laboratories, University of South Australia, Mawson Lakes, South Australia 5095, Australia

ABSTRACT Herein we report a self-cleaning coating derived from zwitterionic poly(2-methacryloyloxylethyl phosphorylcholine) (PMPC) brushes grafted on a solid substrate. The PMPC surface not only exhibits complete oil repellency in a water-wetted state (*i.e.*, underwater superoleophobicity), but also allows effective cleaning of oil fouled on dry surfaces by water alone. The PMPC surface was compared with typical underwater superoleophobic surfaces realized with the aid of surface roughening by applying hydrophilic nanostructures and those realized by applying smooth hydrophilic polyelectrolyte multilayers. We show that underwater superoleophobicity of a surface is not sufficient to enable water to clean up oil fouling on a dry surface, because the latter circumstance demands the surface to be able to strongly bond water not only in its pristine state but also in an oil-wetted state. The PMPC surface is unique with its described self-cleaning performance because the zwitterionic phosphorylcholine groups exhibit exceptional binding affinity to water even when they are already wetted by oil. Further, we show that applying this PMPC coating onto steel meshes produces oil–water separation membranes that are resilient to oil contamination with simply water rinsing. Consequently, we provide an effective solution to the oil contamination issue on the oil–water separation membranes, which is an imperative challenge in this field. Thanks to the self-cleaning effect of the PMPC surface, PMPC-coated steel meshes can not only separate oil from oil–water mixtures in a water-wetted state, but also can lift oil out from oil–water mixtures even in a dry state, which is a very promising technology for practical oil-spill remediation. In contrast, we show that oil contamination on conventional hydrophilic oil–water separation membranes would permanently induce the loss of oil–water separation function, and thus they have to be always used in a completely water-wetted state, which significantly restricts their application in practice.

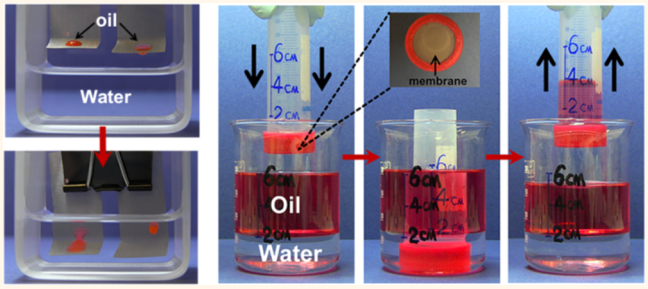

KEYWORDS: self-cleaning · oil–water separation · oil spill remediation · oil cleaning · zwitterionic surface · polymer brush · thin film

Surface cleaning today relies mainly on water action because water is the cheapest, amplest and most environmentally benign solvent. However, water generally experiences difficulties in cleaning up oil contaminants from solid surfaces compared with dust and polar-organic ones. This is because oil has stronger adhesion to common solid surfaces than water due to its smaller surface tension and higher viscosity.[1−4] Thus, effective oil cleaning with water requires a considerable amount of detergents with the help of high mechanical and thermal energy input. The extensive usage of detergents is a profound environmental concern nowadays.[5] Therefore, it will be of great interest and significance to develop a surface on which oil contamination can be cleaned by water alone. To this end, a straightforward approach involves displacing oil by water at the oil–solid interface, which consequently demands that the surface has exceptional binding affinity toward water.

* Address correspondence to xiaokong.liu@unisa.edu.au or liuxiaokong@gmail.com.

Received for review June 22, 2015 and accepted August 10, 2015.

Published online August 10, 2015
10.1021/acsnano.5b03791

Zwitterionic phosphorylcholine (PC), the headgroup of phospholipids that are the main lipid components of cell outer membranes, is reported to be the primary contributor to the "self-cleaning" characteristic of certain cell membranes (*e.g.*, outer membrane of red blood cells), which resist biofouling to keep the membrane surface bioinert.[6−11] It has been experimentally and theoretically demonstrated that the zwitterions integrating both positively and negatively charged units in one group, such as PC, can superiorly bind water molecules *via* electrostatically induced hydration, even compared to those hydrophilic materials to achieve hydration *via* hydrogen bond, such as polyethylene glycol (PEG).[12−16] This is proposed to be the key mechanism for the nonfouling nature of the outer membranes of red blood cells because the tightly bound water layer at the membrane surfaces form a barrier for biofouling.[6−16] As a polymer form of PC, the biomimetic polyelectrolyte, poly(2-methacryloyloxylethyl phosphorylcholine) (PMPC), has been widely used for the fabrication of antibiofouling coatings.[8,14,17] Inspired by the discovery that PC groups endow the outer membranes of red blood cells with the "self-cleaning" nature attributed to their strong water-binding affinity, we found that the zwitterionic PMPC brush surface not only exhibits complete oil-repellency in a water-wetted state, but also, oil fouled on the dry PMPC surface can be completely displaced by water at the oil−solid interface. When an oil-contaminated PMPC surface is immersed in water, spontaneous, rapid and complete oil dewetting is observed and subsequently leaves a clean surface behind.

One important technical application of such a self-cleaning coating is making oil−water separation membranes that are resilient to oil contamination, which is crucial for those used for practical oil spill remediation. There have been two types of oil−water separation membranes reported to date. One is hydrophobic but oleophilic membranes that selectively permit oil to pass through,[18−23] while the other one is hydrophilic membranes that are capable of completely repelling oil in a water-wetted state (*i.e.*, underwater superoleophobicity) and thus selectively allow water to penetrate.[20−30] Compared to the former type of oil−water separation membranes that are easily clogged by viscous oil and consequently lose their oil−water separation function,[22] the latter type of membranes are currently more prevailing because they are oil repellent as long as they are water-wetted. However, the hydrophilic membranes are easily contaminated by oil when dry due to their intrinsic high surface energy.[31,32] The oil contamination is difficult to remove once adsorbed, because of the strong adhesion of oil, and thus leads to the loss of their oil−water separation function as well.[22,25] Accordingly, these hydrophilic oil−water separation membranes have to be always used in a completely water-wetted state and the contact of dry membranes with oil should be strictly avoided, which significantly restricts their application in practice. Therefore, dealing with oil contamination is an imperative challenge for oil−water separation membranes, yet few effective and practical strategies are currently available. Herein, self-cleaning oil−water separation membranes are obtained by grafting PMPC on top of steel meshes. Oil contamination on the membranes can be effectively cleaned up by water, and their oil−water separation function can thus be easily recovered. Meanwhile, thanks to the described self-cleaning effect, the PMPC coated meshes can not only separate oil from oil−water mixtures in a water-wetted state, but also, oil can be selectively lifted out from oil−water mixtures even using the dry PMPC-Mesh, which is a very promising technology for practical oil-spill remediation. Although other zwitterionic polyelectrolytes have been used for the fabrication of oil−water separation membranes with the advantage of not requiring the fabrication of surface roughness,[27−30] attention was only paid to the underwater superoleophobicity of the membranes, which enabled oil−water separation when the membranes were prewetted by water. The issue of oil-contamination on the as-fabricated dry membranes was never investigated nor mentioned, despite it being crucial for practical oil spill remediation. Beyond the extensive study of zwitterionic polymer coatings for antibiofouling surfaces, this is the first known report focusing on their self-cleaning effect that enables oil cleaning with water and their application on oil−water separation membranes that are resilient to oil contamination.

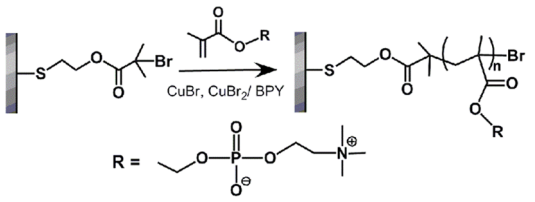

Scheme 1. Schematic Illustration of Grafting PMPC onto a Gold Substrate Modified with Initiators *via* SI-ATRP

RESULTS AND DISCUSSION

For the proof of concept, a model zwitterionic polymer coating was obtained by grafting PMPC brushes with film thickness of *ca.* 20 nm onto gold substrates *via* surface-initiated atom transfer radical polymerization (SI-ATRP). (Scheme 1 and Figure S1). In agreement with a previous report,[33] the PMPC surface is highly hydrophilic with water contact angle in air (WCA-A) of only *ca.* 3°, which is even comparable to the renowned hydrophilic surfaces of Si wafers that are freshly cleaned by Piranha solution (Si-OH) and textured hydrophilic surfaces exampled by steel supported ZnO nanostructures (Nano-ZnO)[34] (Figure 1a and Figure S2). To preliminarily evaluate the water-binding affinity of the PMPC surface, it was challenged by oil

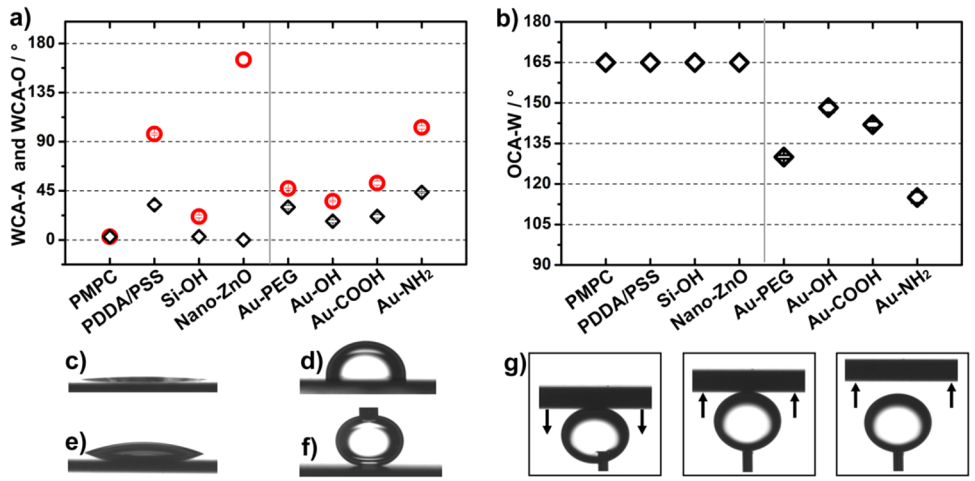

Figure 1. (a,b) Plots of WCA-A (diamonds, a), WCA-O (circles, a) and OCA-W (b) values of various kinds of hydrophilic surfaces. (c–f) photos of 2 μL water droplets on PMPC (c), PDDA/PSS (d), Si-OH (e), Nano-ZnO (f) surfaces that were immersed in *n*-hexadecane. (g) A series of photos taken when the PMPC surface was approaching and leaving a droplet of *n*-hexadecane pending on a needle in water. The oil droplet deformed when pressed by the surface but does not attach to the surface (left). When the surface was retracted, no oil residue was left on the surface (middle and right).

after being immersed into water (Scheme S1a). As shown in Figure 1b and 1g, when the PMPC surface was brought and kept in tight contact with a pendant droplet of *n*-hexadecane, it exhibited an oil contact angle in water (OCA-W) of greater than 165°. Intriguingly, when the surface was retracted, complete oil detachment was observed and no oil residue was left on the surface. The PMPC surface is very flat with root-mean-square (RMS) roughness of only 0.25 nm (Figure S3), thus the surface roughness effect on the surface wettability can be ignored. Therefore, the underwater–oil repellency of the PMPC surface is solely attributed to the intrinsic hydration of the zwitterionic PC groups. It has been reported that zwitterions can superiorly bind water molecules through ion-dipole interactions between the two charged-units and water compared to other hydrophilic species, such as single-charged groups and the oligo-(ethylene glycol).[12−14] Applying sum frequency generation vibrational spectroscopy (SFG), an ordered and tightly immobilized interfacial water layer was detected at the zwitterionic polymer/water interfaces,[35,36] which can well explain the excellent underwater–oil repellency of the PMPC surface observed in our work. Recently, we also reported a roughness-independent underwater–oil-repellent surface derived from a polydiallyldimethylammonium chloride (PDDA)/poly(styrenesulfonate) (PSS) multilayer film (PDDA/PSS) (Figure 1b, Figure S4 and Scheme S3), which is resulted from the hydration of ordered benzenesulfonate groups of PSS in water.[37] The Si-OH and Nano-ZnO surfaces show excellent underwater–oil repellency as well (Figure 1b and Figure S4), which is ascribed to the hydration of hydroxyl groups for the former[37] and the combination role of surface roughness and ZnO hydrophilicity for the latter.[31,32,38] In contrast, although PEG is also a widely used material for antibiofouling surfaces,[14] the surface of PEG brushes obtained *via* self-assembly of thiol-terminated PEG onto gold substrate (Au-PEG) can be easily contaminated by oil in water (Scheme S3 and Figure S5), despite it is underwater oleophobic with an OCA-W of 130.0° (Figure 1b). Additionally, other model hydrophilic surfaces were also taken for comparison, including gold substrates coated with self-assembled monolayers (SAMs) of 6-mercapto-1-hexanol (Au-OH), 11-mercaptoundecanoic acid (Au-COOH) and cysteamine (Au-NH_2) (Scheme S3). It is shown in Figure 1b and Figure S5 that all these surfaces can be contaminated by oil in water although they are underwater oleophobic. To sum up, one can conclude that the pristine PMPC, PDDA/PSS, Si-OH and Nano-ZnO surfaces are unique for their excellent underwater–oil repellency compared with common hydrophilic surfaces, which benefits from their outstanding water-binding affinity induced by intrinsic surface hydration or the surface roughness effect.

It can be envisioned that cleaning up oil contamination fouled on a dry surface by water alone demands the surface to be able to strongly bind water not only in its pristine state, but also when they are already wetted by oil. We here propose the measurement of water wettability on a given surface immersed in oil in terms of water contact angle in oil (WCA-O) (Scheme S1b), to assess the water-binding affinity of the surface in an oil-wetted state and also the capability of water to displace oil at the oil–solid interface. All the above-described hydrophilic surfaces can be aggressively wetted by oil (*n*-hexadecane) in a dry state with an oil contact angle in air of *ca.* 3°. However, as shown in Figure 1a, these surfaces can be well differentiated by their equilibrium WCAs-O, especially for the PMPC,

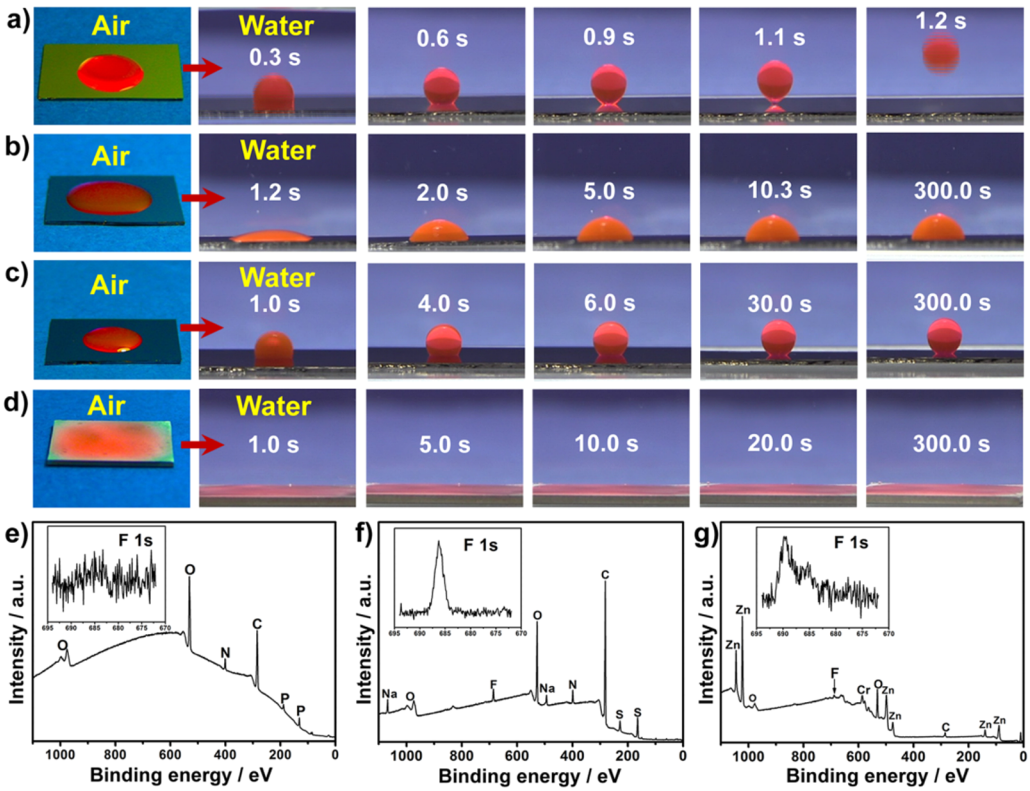

Figure 2. (a–d) Time-lapse photos taken after immersion of the 60 μL canola oil fouled PMPC (a), PDDA/PSS (b), Si-OH (c), Nano-ZnO (d) surface into water. The canola oil was labeled with Nile red. (e–g) XPS wide scan spectra of the PMPC (e), PDDA/PSS (f), Nano-ZnO (g) surface which was first contaminated by Fluorinert FC-70 and then washed by water. The insets are corresponding high-resolution spectra for F element.

PDDA/PSS, Si-OH and Nano-ZnO surfaces that exhibit the same oil-wettability underwater. On the PMPC surface, water droplets can still extensively spread in oil phase with WCA-O as low as its WCA-A, which is *ca.* 3° (Figure 1a and 1c). In contrast, the PDDA/PSS surface is hydrophobic in oil with WCA-O of 100° (Figure 1a and 1d), which is ascribed to the molecular configuration change of the benzenesulfonate groups at interface when immersing in oil.[37] For the Nano-ZnO surface immersed in oil, water droplets are completely repelled with WCA-O above 165° (Figure 1a and 1f), because ZnO nanostructures can effectively trap oil and thus repel water,[39] which is similar to the repellence of water or oil in air by textured surfaces with low surface energy.[40–43] Although the Si-OH surface is shown to be hydrophilic in oil, its WCA-O (*ca.* 21°) is much larger than its WCA-A (Figure 1a and 1e), revealing that oil is harder than air, to be displaced by water at the Si-OH surface. For the cases of Au-PEG, Au-OH, Au-COOH and Au-NH_2 surfaces, their WCAs-O are considerably higher than that of Si-OH surfaces and also their own WCAs-A (Figure 1a), suggesting the difficulty of displacing oil by water at their oil–solid interfaces. Therefore, compared to other hydrophilic surfaces, the exceptional hydrophilicity of PMPC surface in oil phase suggests that the oil-wetted PMPC surface can still superiorly bind water, which also hints the feasibility of displacing oil by water at the oil–solid interface.

To confirm this, we studied dynamic dewetting of oil on a PMPC surface in water. Canola oil that is highly viscous (viscosity of 57 mPa·s at 25 °C) was used as the model of oil, PDDA/PSS, Si-OH and Nano-ZnO surfaces that exhibit the same underwater–oil repellency as PMPC surface were taken as controls. As shown in Figure 2a and Movie S1, when the oil-fouled PMPC surface was immersed into water, the flat oil layer spontaneously shrank into a single droplet and detached from the surface under 1.2 s. Note that a thorough drying of the PMPC surface at 100 °C for 72 h did not have any impact on the underwater–oil dewetting performance. In contrast, immersion of the oil-fouled PDDA/PSS surface into water only induced the oil to shrink into a hemisphere with a contact angle on the surface of *ca.* 90° (Figure 2b). For the Si-OH surface, oil dewetting in water caused the oil layer to shrink into a single droplet within 30s but it was pinned on the surface without detachment (Figure 2c), and a considerable amount of oil was still left on the surface even after vigorous mechanical shaking. Differently from the underwater–oil dewetting on PMPC, PDDA/PSS and Si-OH surfaces, no oil dewetting was observed when the oil-fouled Nano-ZnO surface was immersed in water (Figure 2d), indicating that the oil was firmly trapped by ZnO nanostructures. This result indicates that the surface roughness is a physical obstacle for the underwater–oil dewetting (*i.e.*, cleaning oil

contamination by water) on hydrophilic surfaces. By comparing the underwater–oil dewetting results of these surfaces with their WCAs-O, one can clearly find that the WCA-O of a surface can remarkably implicates the extent to which oil fouled on the surface can be displaced by water at the oil–solid interface.

To explain the displacement of oil by water at the PMPC polymer/oil interface, the following mechanism is proposed. When the zwitterionic PMPC surface is wetted by oil, the dominant interaction between the oil molecules and the polymers is van der Waals interactions,[44–46] while the zwitterions could strongly interact with water through electrostatic induced ion-dipole interactions.[12–14] It is well acknowledged that ion-dipole interaction is longer-ranged and much stronger than van der Waals interaction.[44–46] In addition, it has been reported that a thin precursor liquid film (*i.e.*, typical thickness between 10 nm and a single molecular layer) exists at the edge of a macroscopic liquid drop which spreads out on a solid surface.[47–50] Therefore, when water approaches an oil-wetted PMPC surface, the strong attraction between the PC zwitterions and the water molecules across the thin precursor oil film at the edge of the oil drop spread on the PMPC surface could induce the drainage and a gradual displacement of the oil molecules by water starting from the edge of the oil drop toward the center. The gradual displacement of oil by water would lead to the complete oil-dewetting and detachment of the oil drop from the PMPC surface due to the buoyancy. Direct force measurements using the surface forces apparatus and the atomic force microscope coupled with drop cantilever technique,[51–53] combined with the interfacial molecular configuration analysis using SFG[35,36] will provide quantitative information to verify the proposed mechanism in future work.

The complete oil dewetting on the PMPC surface in water expressly indicates the reality of cleaning up oil fouled on top of it by water. We show in Figure S6 that the PMPC surface which was fully contaminated by Nile red-labeled canola oil can be thoroughly cleaned by water washing as evidenced by the absence of Nile red luminescence under UV light, whereas the oil cannot be cleaned up at all on the pristine gold surface. The self-cleaning effect of PMPC surface is irrespective to the nature of oil. A PMPC surface was fully contaminated by the perfluorinated oil (Fluorinert FC-70) and washed by water (Figure S7), followed by X-ray photoelectron spectroscopy (XPS) analysis. No signal of F can be detected from the water-washed sample (Figure 2e), ascertaining thorough cleaning of the surface by water. In contrast, after the same oil contamination and water washing steps, obvious F signals can still be detected from the PDDA/PSS and Nano-ZnO surfaces (Figure 2f and 2g). Therefore, although all the PMPC, PDDA/PSS and Nano-ZnO surfaces exhibit the same excellent oil repellency in a water-wetted state, while only the PMPC surface enables water to clean oil fouled on its dry state.

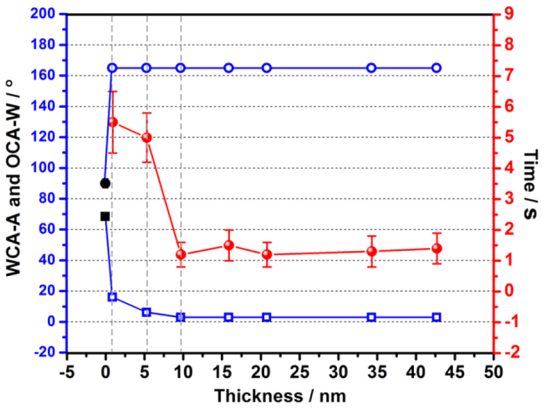

Figure 3. Plots of WCA-A (blue open squares), OCA-W (blue open circles) values and time (red spheres) taken for the complete dewetting of 60 μL canola oil on PMPC surfaces in water as a function of the PMPC film thickness. The black closed square and circle represent the WCA-A and OCA-W on the surfaces of initiator modified gold substrates (see Scheme 1), respectively.

The SI-ATRP allows us to finely control the thickness of as-obtained PMPC films and thus investigate the dependence of their self-cleaning effect on the film thickness. A linear thickness increase of the PMPC film was observed with ATRP time (Figure S8). We show in Figure 3 the PMPC surface wettability (OCA-W and WCA-A) and also the time taken for the complete dewetting of 60 μL canola oil on the surface in water as a function of the PMPC film thickness. The PMPC surfaces with film thickness larger than 0.9 nm obtained from >0.5 h ATRP already exhibit excellent underwater–oil repellency. Meanwhile, all of these surfaces enable water to clean up oil fouled atop, as evidenced by the complete underwater–oil dewetting, despite that is slower on thinner films with thickness of 0.9 nm (5.5 s) and 5.3 nm (5 s) than on those with thickness above 9.7 nm (1.2–1.5 s). This is expected because films formed by shorter polymer brushes are not as dense as those formed by longer ones.[54] Thus, the hydrophobicity of Br atom would contribute more to the surface property, inducing attenuated water-binding affinity, as evidenced by the higher WCAs-A on the films of 0.9 and 5.3 nm thick compared to those on films with thickness above 9.7 nm (Figure 3).

The frequently happened oil spill accidents worldwide have stimulated the boom of developing effective oil–water separation techniques. Using of membranes with hydrophilic coatings that are able to repel oil in a water-wetted state is the prevailing strategy because water can selectively pass through the membrane driven by gravity whereas oil is retained.[20–30] However, hydrophilic membranes are easily fouled by oil in a dry state and thus leads to the loss of oil–water separation function, especially those

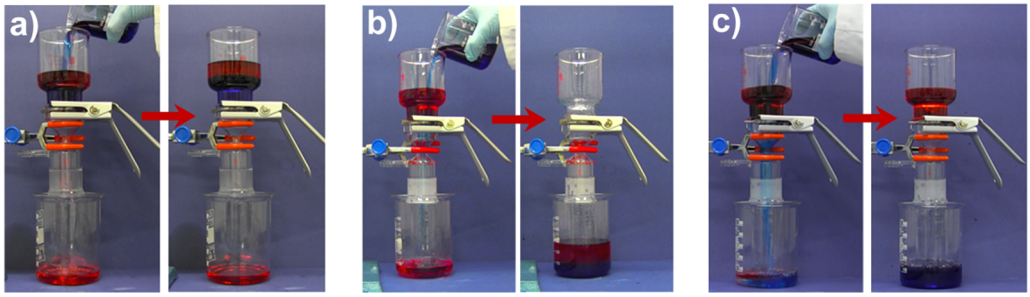

Figure 4. (a,b) Photos shot during filtration of the petroleum-water mixtures through the ZnO-Mesh (a) and PDDA/PSS-Mesh (b), prior to which, the meshes were prewetted by petroleum. (c) Photos shot during filtration of the petroleum-water mixtures through the PMPC-Mesh which was prewetted by petroleum and washed by water rinsing (see Figure S12c). The petroleum was labeled by Oil Red O and water was labeled by methylene blue. The apertures of all the meshes are 100 μm.

with nanostructures that firmly traps oil but are commonly required to make such coatings.[20−26] Herein, the stainless steel meshes coated with ZnO nanostructures (ZnO-Mesh) with thickness of *ca.* 7.8 μm or smooth four bilayers of PDDA/PSS films (PDDA/PSS-Mesh) are taken as examples for the typical hydrophilic oil−water separation membranes derived from textured or smooth underwater superoleophobic coatings, respectively (Figures S9a−d and S11e). As shown in Figure S10a,b, both the ZnO-Mesh and PDDA/PSS-Mesh can effectively separate oil (petroleum, Sigma-Aldrich, product no. 77370) from oil−water mixtures if they were completely prewetted by water. A detailed investigation of the dependence of oil−water separation performance of the water-wetted ZnO-Meshes on the thickness of ZnO coatings is illustrated in the Supporting Information (Figures S11 and S12). Differently from the situation that the ZnO-mesh was prewetted by water, if the ZnO-Mesh was prewetted by oil, neither water nor oil can pass through (Figure 4a), because oil trapped in the ZnO nanostructures cannot undergo any dewetting in water (Figure S13, left sample) and thus prevent water to flow through. Subsequently, water will become the barrier layer of oil owing to its lower density. For the case of PDDA/PSS-Mesh without nanostructures applied, both water and oil can pass through the membrane that was prewetted by oil (Figure 4b). This is because the oil fouled on PDDA/PSS surface can partially dewet in water (Figure S13, right sample), and thus the oil layer supported by the membrane becomes discontinuous, allowing both water and oil to seep through. Additionally, water washing of the oil-wetted ZnO-Mesh and PDDA/PSS-Mesh does not help to recover their oil−water separation function at all (Figure S14a,b).

We grafted PMPC brushes on top of stainless steel meshes with apertures varied from 25, 35, 50 to 100 μm in order to endow the as-obtained membranes with self-cleaning effect (Scheme S2, Figure S9e,f, Figure S15 in the Supporting Information). A set of oil−water separation tests was first performed on the water-wetted PMPC-Meshes with different apertures that were obtained *via* a 12 h polymerization under the same condition as that used for the preparation of PMPC coatings on gold substrates. The thickness of the PMPC coating on the mesh is estimated to be *ca.* 20 nm according to the results measured on the gold substrate (Figure S8). Note that it is difficult to accurately measure the thickness (*i.e.*, nanometers to tens of nanometers) of PMPC coatings on the stainless steel meshes. As expected, after prewetting by water, the PMPC-Meshes can effectively separate oil (petroleum) from the oil−water mixtures by selectively permitting water to pass through (Figure S10c), similar to the behavior of the ZnO-Mesh and PDDA/PSS-Mesh. The retained oil by the water-wetted membrane with underwater superoleophobic coatings is supported by the continuous water layer held by the hydrophilic membrane. It has been reported that there is a threshold of pressure (originated from the oil gravity) the water layer can support, beyond which the oil would break through the membrane.[24] According to the theoretical calculation,[24] the maximum height of oil the membrane can support (*i.e.*, breakthrough height) is decided by the membrane aperture if the OCA-W on the coating of the membrane is the same. As shown in Figure 5a, the breakthrough height of petroleum the PMPC-Meshes can support decreases from *ca.* 60 to *ca.* 45, 32, and 18 cm with an enlargement of the membrane apertures from 25 to 35, 50, and 100 μm. On the contrary, the maximum water fluxes through the membranes increase from *ca.* 616 to *ca.* 685, 838, and 880 L m^{-2} s^{-1} with the enlargement of the membrane aperture from 25 to 35, 50, and 100 μm (Figure 5a). Figure 5b shows the dependence of oil content in water obtained as the filtrate after the filtration of mixtures of 200 mL petroleum and 200 mL water through the PMPC-Meshes on the mesh apertures. The oil content in water obtained from the oil−water separation through the membrane with an aperture of 100 μm is the highest, but was low as 3.2 ppm, which indicates that all the as-prepared PMPC-Meshes exhibit very high oil−water separation efficiency. Furthermore, the oil−water separation performance of the PMPC-Mesh (aperture of 100 μm) obtained *via* a 3 h polymerization was observed to

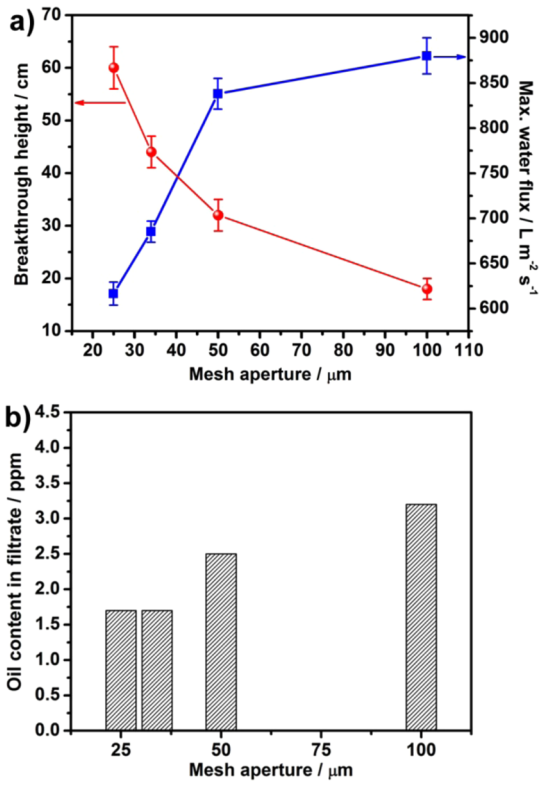

Figure 5. (a) The dependence of the petroleum breakthrough height the PMPC-Meshes can support and the maximum water flux through the PMPC-Meshes on the mesh apertures. (b) The dependence of oil concentration in the filtrate obtained after the filtration of petroleum-water mixtures through the PMPC-Meshes on the mesh apertures. The PMPC-Meshes with apertures varied from 25, 35, 50 to 100 μm were used for the oil–water separation.

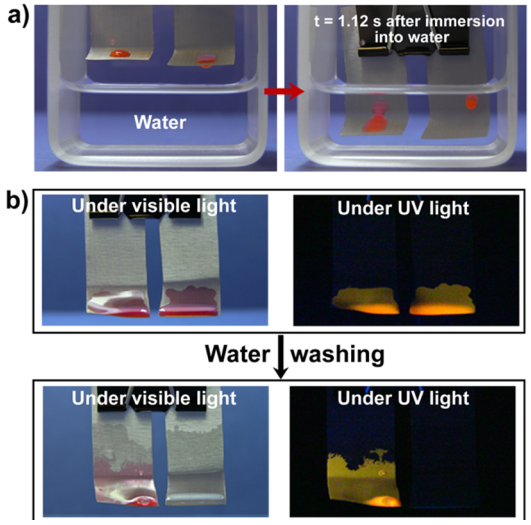

Figure 6. (a) Photos of stainless steel meshes coated without (left sample) and with (right sample) PMPC coatings, fouled by 30 μL Nile red-labeled canola oil in air, before (left panel) and after (right panel) being immersed into water. (b) Photos, taken under visible (left panels) and UV (right panels) light, of the stainless steel meshes coated without (left sample) and with (right sample) PMPC coatings, fouled by Nile red-labeled canola oil in air, before (upper panels) and after (lower panels) being washed by water alone. It can be observed that the oil fouled on the PMPC-coated mesh can be thoroughly cleaned by water washing, as evidenced by the absence of luminescence of Nile red under UV light. The apertures of the meshes are 100 μm and the PMPC coating thickness is estimated to be *ca.* 20 nm.

have little difference compared to that obtained *via* a 12 h polymerization, in terms of the oil breakthrough height, maximum water flux and water (*i.e.*, the filtrate) purity, though the thickness of the as-prepared PMPC coating is estimated to be only *ca.* 5 nm. More importantly, the oil (*e.g.*, canola oil, 30 μL) that was labeled by Nile red and fouled on the dry PMPC-Mesh with aperture of 100 μm underwent complete dewetting and detachment in only 1.1 s when being immersed into water (Figure 6a, Movie S2), which enabled a thoroughly cleaning of the oil fouled on the PMPC-Mesh by water washing (Figure 6b). The described self-cleaning effect of the PMPC-Mesh is irrespective to the mesh apertures. Figure S16 shows the rapid underwater–oil (canola oil, 30 μL) dewetting and detachment (1.1 s was taken) from the PMPC-Mesh with aperture of 25 μm and PMPC coating of *ca.* 20 nm thickness. The PMPC-Mesh with thinner PMPC coatings of only *ca.* 5 nm thickness also exhibits the same self-cleaning effect, though the underwater–oil dewetting and detachment takes longer time (*i.e.*, 11.4 s for 30 μL canola oil) (Figure S17), which is in good agreement with the results observed from the PMPC coatings prepared on flat gold substrates (Figure 3). Thanks to this self-cleaning effect, even if the dry PMPC-Mesh is contaminated by oil, its oil–water separation function can be simply recovered by water washing (Figures 4c and S14c, note that the petroleum observed in the collection beaker in Figure 4c was from that used for oil prewetting). It is worthwhile to note that hydrophilic oil–water separation membranes that are resilient to oil contamination by such a simple and practical treatment have never been achieved before.

In practical oil-spill remediation, the oil–water separation membrane will come into contact with oil first then water because oil tends to float above water. Consequently, the oil contamination on the membrane is hardly evited, which limits the application of conventional hydrophilic oil–water separation membranes that can repel oil only in a water-wetted state. In this context, PMPC-Mesh can be a solution to the challenging issue. Figure 7a and Movie S3 show the mimic of practical oil-spill remediation by using PMPC-Mesh with an aperture of 100 μm and PMPC coating of *ca.* 20 nm thickness. Although the PMPC-Mesh that covers the bottom end of the plastic tube (see inset of Figure 7a$_2$, Figure S18) can be contaminated when going across the oil (petroleum) layer, further lowering the membrane down to the water phase (Figure 7a$_2$) can cause the oil contamination to be displaced by water, as illustrated in Figure 6 and Movie S2. Meanwhile, a continuous water layer can be formed in the membrane as a barrier to prevent oil flow when the

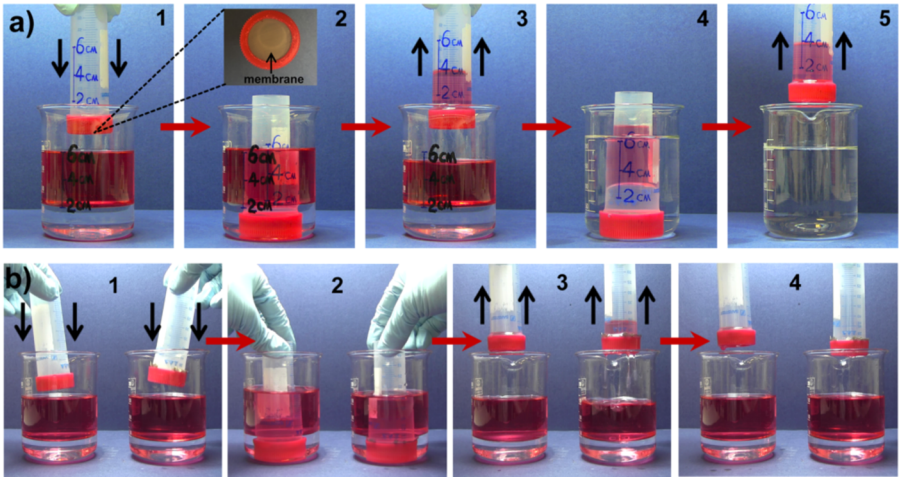

Figure 7. (a) A series of photos captured during the lifting of petroleum out from a petroleum-water mixture by using a plastic tube with the bottom end covered with a PMPC-Mesh (see inset of (a_2) and Figure S18 in Supporting Information). (a_1) The tube was being inserted into the petroleum-water mixture, comprising of 4 cm height of petroleum (the red part) and 2 cm height of water (the colorless part). (a_2) The mesh reached the water phase. (a_3) The tube was lifted out from the petroleum-water mixture. It can be seen that petroleum with height of 4 cm was lifted out and held in the tube. (a_4) The tube holding petroleum shown in (a_3) was transferred into water. (a_5) The tube shown in (a_4) was lifted out into air. It was observed in (a_4) that water can pass through the membrane and thus jack up the petroleum, and in (a_5) that petroleum can still be held in the tube after it was lifted out into air. The graduation labeled on the beaker and plastic tube indicates the height measured from their bottom. (b) A series of photos captured during the insertion of two plastic tubes with their bottom ends respectively covered with ZnO-Mesh (left) and PDDA/PSS-Mesh (right) into the petroleum-water mixtures and then being lifted out into air. (b_1) The tubes were being inserted into the petroleum-water mixtures. (b_2) The meshes reached the water phases. (b_3) The tubes were lifted out from the petroleum-water mixtures. (b_4) The tubes were held in air for a while. It was observed that neither the ZnO-Mesh nor PDDA/PSS-Mesh can lift petroleum out from the petroleum-water mixture. The petroleum was labeled by Oil Red O. The apertures of all the meshes are 100 μm.

membrane is lifted out, which subsequently enables the plastic tube to lift oil out from the oil–water mixture (Figure 7a_3). Note that the height of oil lifted out by the PMPC-Mesh-covered plastic tube (Figure 7a_3) is the same as that of the original oil–water mixture (Figure 7a_1). The oil held in the plastic tube is supported by a continuous water layer can be further evidenced by the fact that water can freely transport through the membrane but oil is always retained (Figure 7a_4, 7a_5, and Movie S3). In addition, the dry PMPC-Mesh (aperture of 100 μm) with the PMPC coating of *ca.* 5 nm thickness can also exhibit the same performance. In contrast, neither the ZnO-Mesh nor PDDA/PSS-mesh can be effective for lifting oil out from oil–water mixtures (Figure 7b, Movie S4). For the ZnO-Mesh, once it is contaminated by oil when moving across the oil layer, water cannot pass through the membrane because ZnO nanostructures with trapped oil will completely repel water (Figure 1f). Subsequently, when the membrane is lifted out, oil will naturally flow out from the membrane driven by gravity (Figure 7b_3 and 7b_4). In the case of the PDDA/PSS-Mesh, when the oil-contaminated membrane immerses into the water phase, water can pass though because of the partial dewetting of oil in water implicated in Figure S13. However, the oil cannot be removed but stays in form of droplets, which prevents the formation of continuous water layer in the membrane. Consequently, the oil cannot be held when the membrane is lifted out, it flows out instead (Figure 7b_3 and 7b_4). Furthermore, we show in Movie S5 that the PMPC-Mesh can also selectively lift crude oil out from crude-oil seawater mixtures, which illustrates the feasibility of using PMPC-Mesh for practical oil-spill remediation.

CONCLUSIONS

In summary, we have demonstrated that the zwitterionic PMPC surface exhibits not only the self-cleaning effect against oil fouling in a water-wetted state, but also that oil fouled on the dry PMPC surfaces can be cleaned up by water alone. The exceptional water-binding affinity of the zwitterionic PC groups in their pristine and even oil-wetted states gives rise to the self-cleaning effect of the PMPC surface. This new concept of self-cleaning provides an alternative to making oil-repellent surfaces *via* minimizing oil wetting,[40–43] which is generally difficult to be realized in practice. Applying the PMPC coating onto steel meshes enables us to create oil–water separation membranes that are resilient to oil contamination when simply rinsed with water. In addition, even dry PMPC coated meshes can selectively lift oil out from oil–water mixtures, which is a promising remediation for oil spills. Our ongoing effort is devoted to understand the origin of the superior water-binding affinity of zwitterions and also the parameters that affects this unique property. This knowledge will be helpful to generalize and simplify the preparation of self-cleaning coatings based on the

zwitterionic species. Thanks to the development of simple polymerization techniques, especially the grafting of polymer brushes *via* ATRP at ambient atmosphere,[55,56] we believe that the self-cleaning zwitterionic polymer coatings can be readily applied in practice.

EXPERIMENTAL SECTION

Materials. Bis(2-hydroxyethyl) disulfide (90%), 2-bromo-2-methylpropionyl bromide (98%), triethylamine (99%), 2-bromo-2-methylpropionic acid (98%), *N*,*N*′-dicyclohexylcarbodiimide (DCC, 99%), 4-(dimethylamino)pyridine (DMAP, ≥ 99%), (3-aminopropyl)triethoxysilane (APTS) (99%), 2-methacryloyloxyethyl phosphorylcholine (97%), 2,2′-bipyridyl (BPY, ≥ 99%), methyl 2-bromopropionate (MBP, 98%), copper(I) bromide (98%) copper(II) bromide (99%), dichloromethane (anhydrous, ≥ 99.8%), 11-mercaptoundecanoic acid (HS-C10-COOH), cysteamine (HS-C2-NH_2), poly(ethylene glycol) methyl ether thiol (M_n of *ca.* 2000) (HS-PEG), 6-mercapto-1-hexanol (97%) (HS-C6-OH), Poly(diallyldimethylammonium chloride) solution (PDDA, 20% in water, M_W 100 000−200 000), Poly(sodium 4-styrenesulfonate) (PSS, M_W 70000), zinc acetate dihydrate ($Zn(CH_3COO)_2$) (≥98%), hexadecane (99%), petroleum (special, ∼ 18% aromatics basis), Nile red, Oil Red O, Fluorinert FC-70, were purchased from Sigma-Aldrich. Ethanol, ammonium hydroxide solution, acetone, and isopropanol, all in AR grade, were purchased from Chem-Supply, Australia. Canola oil, produced by Wintercorn Edible, Australia, was purchased from a local supermarket. Copper(I) bromide (98%) was purified by stirring in glacial acetic acid, followed by rinsing with ethanol and drying in a vacuum. Other chemicals were used as received without further purification. Steel plates were kindly supplied by the workshop of Ian Wark Research Institute, University of South Australia. Crude oil was kindly supplied by China Petrochemical Corporation (SHENGLI Oilfields), seawater was collected from Semaphore beach in Adelaide, South Australia. The water with a resistivity of >18.2 MΩ was used for all the experiments. Si wafers were purchased from Si-Mat Silicon Materials, Germany. Gold coated Si wafers were prepared by consecutive electron beam evaporation of chromium layers of 10 nm thick and gold layers of 50 nm thick on silicon wafers. Prior to further surface modification, the gold-coated Si wafers were exposed to ozone for 30 min in a UV/ozone cleaner at room temperature. Stainless steel meshes with aperture of 100 μm made of Stainless Steel T316 were purchased from Sefar, Australia.

Synthesis of Bis[2-(2′-bromoisobutyryloxy) ethyl] Disulfide (BEDS). BEDS was synthesized by acrylation of bis(2-hydroxyethyl) disulfide with 2-bromoisobutyryl bromide in the presence of triethylamine by using a procedure described in the literature.[57] The obtained BEDS will be used as initiator for the preparation of PMPC brushes on gold substrates.

Preparation of PMPC Coatings on Gold Substrates. (i) Initiator immobilization: The cleaned gold-coated Si wafers were immersed in the ethanol solution of BEDS (1 mM) for 24 h, then rinsed with ethanol and dried by N_2 flow. (ii) Preparation of PMPC brushes on gold substrates *via* surface-initiated atom transfer radical polymerization (SI-ATRP): Typically, a 25 mL flask was charged with 2-methacryloyloxyethyl phosphorylcholine (1.25 g, 4.23 mmol), 2,2′-bipyridyl (0.0309 g, 0.198 mmol) and 3 mL of methanol. The gold substrate with initiator (BEDS) immobilized was immersed into the reactant solution. 11.6 μL of methanol solution of MBP with a MBP concentration of 0.90 M was added to the flask. The flask was then sealed and degassed using the freeze−thaw method for 3 cycles and afterward filled with argon. Subsequently, the sealed flask was opened and a catalyst containing CuBr (0.0101 g, 0.0704 mmol) and $CuBr_2$ (0.005 g, 0.0224 mmol) was rapidly added into the flask which was kept in liquid nitrogen. Then the flask was sealed again, followed by degassing using the freeze−thaw method for another 3 cycles and finally filled with argon. The flask was then incubated in a water bath under stirring at 30 °C. The polymerization was terminated by exposing the system to air at desired polymerization time. The obtained PMPC-grafted gold substrate was rinsed by ethanol and water, followed by drying with N_2 flow.

Preparation of Si-OH, PDDA/PSS and Nano-ZnO Surfaces. (i) Si-OH surfaces were prepared by immersing silicon wafers into Piranha solution (1:3 (v/v) mixture of 30% H_2O_2 and 98% H_2SO_4), followed by heating until no bubbles were released. *Caution! Piranha solution reacts violently with organic materials and should be handled carefully.* Afterward, the wafers were thoroughly rinsed with water, dried with N_2 flow, and used for further experiments immediately. (ii) PDDA/PSS surfaces were prepared by alternate deposition of PDDA and PSS on Piranha solution cleaned Si substrates for 4 cycles.[37] In the PDDA or PSS solution, the concentration of PDDA or PSS is 1.0 mg/mL and the concentration of NaCl is 1.0 M. (iii) Nano-ZnO surfaces were obtained by growing ZnO nanostructures on steel plates (25 mm × 18 mm) by using the protocol reported in the literature.[34] Typically, the stainless steel plates were first incubated in HNO_3 solution (4 M) at 60 °C for 4h, followed by sonication with water, 2-propanol and ethanol for 10 min, respectively, and finally they were dried by N_2 flow. An aqueous precursor solution was prepared by dissolving $Zn(CH_3COO)_2$ into water to make the $Zn(CH_3COO)_2$ concentration of 0.0125 M, followed by adjusting the pH of the $Zn(CH_3COO)_2$ solution to 10.35 *via* dropwise adding ammonia solution (28%). The precursor solution was then transferred into a laboratory bottle and the HNO_3 treated stainless steel plates were then incubated into the solution. The laboratory bottle was then sealed and incubated in an oil bath at 95 °C for 5h. Finally, the stainless steel plates were taken out, followed by thorough water rinsing and drying by N_2 flow.

Preparation of Au-PEG, Au-OH, Au-COOH, and Au-NH_2 Surfaces. (i) Au-PEG and Au-NH_2 surfaces were prepared by incubation of cleaned gold-coated Si wafers into aqueous solutions of HS-C2-NH_2 (2.5 mM) and HS-PEG (1 mg/mL), respectively, for 24 h at room temperature, followed by thorough rinsing with water and drying with N_2 flow. (ii) Au-COOH and Au-OH surfaces were prepared by incubation of cleaned gold-coated Si wafers into the ethanol solutions of HS-C10-COOH (1 mM) and HS-C6-OH (1 mM), respectively, for 24 h at room temperature, followed by thorough rinsing with ethanol and drying with N_2 flow.

Preparation of PMPC Brushes on Si Substrates. (i) Initiator immobilization. The freshly obtained Piranha solution cleaned Si wafers were further dried at 80 °C for 1 h. The dried silicon wafers were first modified with APTS *via* chemical vapor deposition (CVD) following the previously reported procedures.[58] After rinsing with ethanol and drying with N_2 flow, the APTS modified Si wafers were immersed into a solution of anhydrous dichloromethane (10 mL) containing 2-bromo-2-methylpropionic acid (0.02 M), DMAP (0.005 M). The solution was then cooled to 0 °C and DCC was added to make a final concentration of 0.025 M. After DCC was dissolved, the solution was left overnight at room temperature. The obtained Si wafers were rinsed with toluene and acetone and dried with N_2 flow. (ii) Preparation of PMPC coatings on Si substrates *via* SI-ATRP. The same procedures were followed as that used for preparation of PMPC coatings on gold substrates.

Preparation of Oil−Water Separation Membranes by Using Stainless Steel Meshes. (i) PMPC-Mesh. PMPC brushes were grafted on stainless steel meshes following the same procedures used for the grafting of PMPC on Si substrates. (ii) PDDA/PSS-Mesh. PDDA/PSS multilayers with 4 bilayers were grown on the stainless steel meshes following the same procedures used for preparation of PDDA/PSS multilayers on Si substrates. (iii) ZnO-mesh. ZnO nanostructures were grown on stainless steel meshes following the same procedures used for preparation of Nano-ZnO surfaces.

Characterization. Contact angle measurements were completed on a Dataphysics OCA 20 contact angle system at ambient temperature using a 2 μL liquid droplet as indicator. Colorimeter glass cells, purchased from Starna, were used for oil

contact angle in water (OCA-W) measurements. Atomic force microscopy (AFM) imaging was performed with a MultiMode 8 AFM from Bruker in a ScanAsyst mode at ambient condition using Si cantilevers. X-ray photoelectron spectroscopy (XPS) was carried out on a Kratos Axis Ultra with a Delay Line Detector photoelectron spectrometer using an Aluminum monochromatic X-ray source. The thicknesses of the PMPC films were determined by using a J. A. Woolham Co. V-VASE spectroscopic ellipsometer. Three different spots were measured at three different angles of incidence (65°, 70°, 75°). The thickness of the polymer brush was determined using the Cauchy layer model with an assumed refractive index of 1.45. Scanning electron microscopy (SEM) images were obtained on FEI Quanta 450 operated at 10−20 kV. Oil content in the collected water after oil−water separation was determined by the Agilent 7890A GC system equipped with an Agilent 5975C Mass Selective Detector and Agilent 7890A GC equipped with a Flame Ionization Detector. Digital camera images were captured by using a Canon camera (IXUS100 IS) or a Canon digital video camera (Legria HF G10). Digital videos were taken by a Canon digital video camera (Legria HF G10).

Conflict of Interest: The authors declare no competing financial interest.

Acknowledgment. X. L. thanks the State Government of South Australia and ITEK Ventures Pty Ltd. for the Research Connections Grant (RC44943); D. W. thanks the Australian Research Council (DP120102959).

Supporting Information Available: The Supporting Information is available free of charge on the ACS Publications website at DOI: 10.1021/acsnano.5b03791.

Supplementary Schemes and Figures. XPS analysis of the PMPC surface on a gold substrate (Figure S1), SEM image of the Nano-ZnO surface on a steel substrate (Figure S2), schemetic illustration of the measurement of OCA-W and WCA-O (Scheme S1), AFM image of the PMPC surface on Si substrate (Figure S3), schemetic illustration the process of grafting PMPC brushes onto a Si substrate or a stainless steel mesh (Scheme S2), schemetic illustration the molecular structures of PDDA, PSS and all the thiols used in this study (Scheme S3), study of oil droplet adhesion onto the PDDA/PSS, Si-OH and Nano-ZnO surfaces underwater (Figure S4), oil wettability on Au-PEG, Au-OH, Au-COOH and Au-NH_2 surfaces underwater (Figure S5), illustration of the effective cleaning of oil fouled on the dry PMPC surface by water alone (Figure S6 and S7), thickness increment of the PMPC film with ATRP time (Figure S8), SEM images of the ZnO-Mesh, PDDA/PSS-Mesh and PMPC-Mesh (Figure S9), illustration of the oil−water separation function of the ZnO-Mesh, PDDA/PSS-Mesh and PMPC-Mesh that were prewetted by water (Figure S10), SEM images of the ZnO-Meshes with different ZnO coating thickness (Figure S11), the dependence of oil−water separation performance of the ZnO-meshes on the thickness of ZnO coatings (Figure S12), illustration of the oil dewetting when oil contaminated ZnO-Mesh and PDDA/PSS-mesh were immersed into water (Figure S13), illustration of the oil−water separation function of the ZnO-Mesh, PDDA/PSS-Mesh and PMPC-Mesh that were prewetted by oil followed by water rinsing (Figure S14), XPS analysis of the PMPC-Mesh (Figure S15), illustration of the oil dewetting when oil contaminated PMPC-Meshes with different apertures and different PMPC coating thickness were immersed into water (Figures S16 and S17), illustration of how to cover one end of a plastic tube with a coated steel mesh (Figure S18). (PDF)
Movie S1. (AVI)
Movie S2. (AVI)
Movie S3. (AVI)
Movie S4. (AVI)
Movie S5. (AVI)

REFERENCES AND NOTES

1. Shikhmurzaev, Y. D. Moving Contact Lines in Liquid/Liquid/Solid Systems. *J. Fluid Mech.* **1997**, *334*, 211–249.
2. Blake, T. D. The Physics of Moving Wetting Lines. *J. Colloid Interface Sci.* **2006**, *299*, 1–13.
3. Quéré, D. Wetting and Roughness. *Annu. Rev. Mater. Res.* **2008**, *38*, 71–79.
4. Ramiasa, M.; Ralston, J.; Fetzer, R.; Sedev, R. Contact Line Friction in Liquid-Liquid Displacement on Hydrophobic Surfaces. *J. Phys. Chem. C* **2011**, *115*, 24975–24986.
5. *Handbook of Detergents, Part B: Environmental Impact*; Zoller, U., Ed.; Taylor and Francis: New York, 2004.
6. Zwaal, R. F. A.; Schroit, A. J. Pathophysiologic Implications of Membrane Phospholipid Asymmetry in Blood Cells. *Blood* **1997**, *89*, 1121–1132.
7. Sin, M.-C.; Chen, S.-H.; Chang, Y. Hemocompatibility of Zwitterionic Interfaces and Membranes. *Polym. J.* **2014**, *46*, 436–443.
8. Lewis, A. L. Phosphorylcholine-Based Polymers and Their Use in the Prevention of Biofouling. *Colloids Surf., B* **2000**, *18*, 261–275.
9. Vermette, P.; Meagher, L. Interactions of Phospholipid- and Poly(ethylene glycol)-Modified Surfaces with Biological Systems: Relation to Physico-Chemical Properties and Mechanisms. *Colloids Surf., B* **2003**, *28*, 153–198.
10. Ishihara, K.; Fukumoto, K.; Iwasaki, Y.; Nakabayashi, N. Modification of Polysulfone with Phospholipid Polymer for Improvement of the Blood Compatibility. Part 1. Surface Characterization. *Biomaterials* **1999**, *20*, 1545–1551.
11. Chen, S.; Zheng, J.; Li, L.; Jiang, S. Strong Resistance of Phosphorylcholine Self Assembled Monolayers to Protein Adsorption: Insights into Nonfouling Properties of Zwitterionic Materials. *J. Am. Chem. Soc.* **2005**, *127*, 14473–14478.
12. Hower, J. C.; Bernards, M. T.; Chen, S.; Tsao, H.-K.; Sheng, Y.-J.; Jiang, S. Hydration of "Nonfouling" Functional Groups. *J. Phys. Chem. B* **2009**, *113*, 197–201.
13. He, Y.; Hower, J.; Chen, S.; Bernards, M. T.; Chang, Y.; Jiang, S. Molecular Simulation Studies of Protein Interactions with Zwitterionic Phosphorylcholine Self-Assembled Monolayers in the Presence of Water. *Langmuir* **2008**, *24*, 10358–10364.
14. Chen, S.; Li, L.; Zhao, C.; Zheng, J. Surface Hydration: Principles and Applications toward Low-Fouling/Nonfouling Biomaterials. *Polymer* **2010**, *51*, 5283–5293.
15. Jiang, S.; Cao, Z. Ultralow-Fouling, Functionalizable, and Hydrolyzable Zwitterionic Materials and Their Derivatives for Biological Applications. *Adv. Mater.* **2010**, *22*, 920–932.
16. Schlenoff, J. B. Zwitteration: Coating Surfaces with Zwitterionic Functionality to Reduce Nonspecific Adsorption. *Langmuir* **2014**, *30*, 9625–9636.
17. Yang, W. J.; Cai, T.; Neoh, K.-G.; Kang, E.-T.; Teo, S. L.-M.; Rittschof, D. Barnacle Cement as Surface Anchor for "Clicking" of Antifouling and Antimicrobial Polymer Brushes on Stainless Steel. *Biomacromolecules* **2013**, *14*, 2041–2051.
18. Feng, L.; Zhang, Z.; Mai, Z.; Ma, Y.; Liu, B.; Jiang, L.; Zhu, D. A Super-Hydrophobic and Super-Oleophilic Coating Mesh Film for the Separation of Oil and Water. *Angew. Chem., Int. Ed.* **2004**, *43*, 2012–2014.
19. Zhang, J.; Seeger, S. Polyester Materials with Superwetting Silicone Nanofilaments for Oil/Water Separation and Selective Oil Absorption. *Adv. Funct. Mater.* **2011**, *21*, 4699–4704.
20. Zhu, Y.; Wang, D.; Jiang, L.; Jin, J. Recent Progress in Developing Advanced Membranes for Emulsified Oil/Water Separation. *NPG Asia Mater.* **2014**, *6*, e101.
21. Wang, B.; Liang, W.; Guo, Z.; Liu, W. Biomimetic Super-Lyophobic and Super-Lyophilic Materials Applied for Oil/Water Separation: A New Strategy Beyond Nature. *Chem. Soc. Rev.* **2015**, *44*, 336–361.
22. Chu, Z.; Feng, Y.; Seeger, S. Oil/Water Separation with Selective Superantiwetting/Superwetting Surface Materials. *Angew. Chem., Int. Ed.* **2015**, *54*, 2328–2338.
23. Zhang, L.; Zhang, Z.; Wang, P. Smart Surfaces with Switchable Superoleophilicity and Superoleophobicity in Aqueous Media: toward Controllable Oil/Water Separation. *NPG Asia Mater.* **2012**, *4*, e8.

24. Xue, Z.; Wang, S.; Lin, L.; Chen, L.; Liu, M.; Feng, L.; Jiang, L. A Novel Superhydrophilic and Underwater Superoleophobic Hydrogel-Coated Mesh for Oil/Water Separation. *Adv. Mater.* **2011**, *23*, 4270–4273.
25. Zhang, L.; Zhong, Y.; Cha, D.; Wang, P. A Self-Cleaning Underwater Superoleophobic Mesh for Oil-Water Separation. *Sci. Rep.* **2013**, *3*, 2326.
26. Gao, S. J.; Shi, Z.; Zhang, W. B.; Zhang, F.; Jin, J. Photoinduced Superwetting Single-Walled Carbon Nanotube/TiO_2 Ultrathin Network Films for Ultrafast Separation of Oil-in-Water Emulsions. *ACS Nano* **2014**, *8*, 6344–6352.
27. Zhu, Y.; Zhang, F.; Wang, D.; Pei, X. F.; Zhang, W.; Jin, J. A Novel Zwitterionic Polyelectrolyte Grafted PVDF Membrane for Thoroughly Separating Oil from Water with Ultrahigh efficiency. *J. Mater. Chem. A* **2013**, *1*, 5758–5765.
28. Liu, Q.; Patel, A. A.; Liu, L. Superhydrophilic and Underwater Superoleophobic Poly(sulfobetaine methacrylate)-Grafted Glass Fiber Filters for Oil-Water Separation. *ACS Appl. Mater. Interfaces* **2014**, *6*, 8996–9003.
29. Yang, R.; Moni, P.; Gleason, K. K. Ultrathin Zwitterionic Coatings for Roughness- independent Underwater Superoleophobicity and Gravity-Driven Oil-Water Separation. *Adv. Mater. Interfaces* **2015**, *2*, 1400489.
30. Ren, P.-F.; Yang, H.-C.; Jin, Y.-N.; Liang, H.-Q.; Wan, L.-S.; Xu, Z.-K. Underwater Superoleophobic Meshes Fabricated by Poly(sulfobetaine)/Polydopamine Co-Deposition. *RSC Adv.* **2015**, *5*, 47592–47598.
31. Liu, M.; Wang, S.; Wei, Z.; Song, Y.; Jiang, L. Bioinspired Design of a Superoleophobic and Low Adhesive Water/Solid Interface. *Adv. Mater.* **2009**, *21*, 665–669.
32. Jung, Y. C.; Bhushan, B. Wetting Behavior of Water and Oil Droplets in Three-Phase Interfaces for Hydrophobicity/philicity and Oleophobicity/philicity. *Langmuir* **2009**, *25*, 14165–14173.
33. Yang, B.; Duan, X.; Huang, J. Ultrathin, Biomimetic, Superhydrophilic Layers of Cross-Linked Poly(phosphobetaine) on Polyethylene by Photografting. *Langmuir* **2015**, *31*, 1120–1126.
34. Bai, W.; Yu, K.; Zhang, Q.; Zhu, X.; Peng, D.; Zhu, Z.; Dai, N.; Sun, Y. Large-Scale Synthesis of Zinc Oxide Rose-Like Structures and Their Optical Properties. *Phys. E* **2008**, *40*, 822–827.
35. Leng, C.; Han, X.; Shao, Q.; Zhu, Y.; Li, Y.; Jiang, S.; Chen, Z. *In Situ* Probing of the Surface Hydration of Zwitterionic Polymer Brushes: Structural and Environmental Effects. *J. Phys. Chem. C* **2014**, *118*, 15840–15845.
36. Leng, C.; Hung, H.-C.; Sieggreen, O. A.; Li, Y.; Jiang, S.; Chen, Z. Probing the Surface Hydration of Nonfouling Zwitterionic and Poly(ethylene glycol) Materials with Isotopic Dilution Spectroscopy. *J. Phys. Chem. C* **2015**, *119*, 8775–8780.
37. Liu, X.; Leng, C.; Yu, L.; He, K.; Brown, L. J.; Chen, Z.; Cho, J.; Wang, D. Ion-Specific Oil Repellency of Polyelectrolyte Multilayers in Water: Molecular Insights into the Hydrophilicity of Charged Surfaces. *Angew. Chem., Int. Ed.* **2015**, *54*, 4851–4856.
38. Liu, X.; Gao, J.; Xue, Z.; Chen, L.; Lin, L.; Jiang, L.; Wang, S. Bioinspired Oil Strider Floating at the Oil/Water Interface Supported by Huge Superoleophobic Force. *ACS Nano* **2012**, *6*, 5614–5620.
39. Tao, M.; Xue, L.; Liu, F.; Jiang, L. An Intelligent Superwetting PVDF Membrane Showing Switchable Transport Performance for Oil/Water Separation. *Adv. Mater.* **2014**, *26*, 2943–2948.
40. Tuteja, A.; Choi, W.; Ma, M.; Mabry, J. M.; Mazzella, S. A.; Rutledge, G. C.; McKinley, G. H.; Cohen, R. E. Designing Superoleophobic Surfaces. *Science* **2007**, *318*, 1618–1622.
41. Pan, S.; Kota, A. K.; Mabry, J. M.; Tuteja, A. Superomniphobic Surfaces for Effective Chemical Shielding. *J. Am. Chem. Soc.* **2013**, *135*, 578–581.
42. Deng, X.; Mammen, L.; Butt, H.-J.; Vollmer, D. Candle Soot as a Template for a Transparent Robust Superamphiphobic Coating. *Science* **2012**, *335*, 67–70.
43. Zhang, J.; Seeger, S. Superoleophobic Coatings with Ultralow Sliding Angles Based on Silicone Nanofilaments. *Angew. Chem., Int. Ed.* **2011**, *50*, 6652–6656.
44. Margenau, H.; Kestner, N. *Theory of Intermolecular Forces*, 2nd ed.; Pergamon Press Ltd.: Oxford, 1971.
45. Schalley, C. A. *Analytical Methods in Supramolecular Chemistry*; Schalley, C., Ed.; Wiley-VCH Verlag GmbH & Co. KGaA: Weinheim, 2007; Chapter 1, pp 1−16.
46. Israelachvili, J. *Intermolecular and Surface Forces*, 3rd ed.; Academic Press: Waltham, MA, 2011.
47. Cazabat, A.-M.; Gerdes, S.; Valignat, M. P.; Villette, S. Dynamics of Wetting: From Theory to Experiment. *Interface Sci.* **1997**, *5*, 129–139.
48. Kavehpour, H. P.; Ovryn, B.; McKinley, G. H. Evaporatively-Driven Marangoni Instabilities of Volatile Liquid Films Spreading on Thermally Active Substrates. *Colloids Surf., A* **2002**, *206*, 409.
49. Bonn, D.; Eggers, J.; Indekeu, J.; Meunier, J.; Rolley, E. Wetting and Spreading. *Rev. Mod. Phys.* **2009**, *81*, 739–805.
50. Zeng, H.; Tian, Y.; Zhao, B.; Tirrell, M.; Israelachvili, J. Transient Interfacial Patterns and Instabilities Associated with Liquid Film Adhesion and Spreading. *Langmuir* **2007**, *23*, 6126–6135.
51. Shi, C.; Cui, X.; Xie, L.; Liu, Q.; Chan, D. Y. C.; Israelachvili, J. N.; Zeng, H. Measuring Forces and Spatiotemporal Evolution of Thin Water Films between an Air Bubble and Solid Surfaces of Different Hydrophobicity. *ACS Nano* **2015**, *9*, 95–104.
52. Shi, C.; Chan, D. Y. C.; Liu, Q.; Zeng, H. Probing the Hydrophobic Interaction between Air Bubbles and Partially Hydrophobic Surfaces Using Atomic Force Microscopy. *J. Phys. Chem. C* **2014**, *118*, 25000–25008.
53. Faghihnejad, A.; Zeng, H. Hydrophobic Interactions between Polymer Surfaces: Using Polystyrene as a Model System. *Soft Matter* **2012**, *8*, 2746–2759.
54. Yang, W.; Chen, S.; Cheng, G.; Vaisocherová, H.; Xue, H.; Li, W.; Zhang, J.; Jiang, S. Film Thickness Dependence of Protein Adsorption from Blood Serum and Plasma onto Poly(sulfobetaine)-Grafted Surfaces. *Langmuir* **2008**, *24*, 9211–9214.
55. Yan, J.; Li, B.; Yu, B.; Huck, W. T. S.; Liu, W.; Zhou, F. Controlled Polymer-Brush Growth from Microliter Volumes using Sacrificial-Anode Atom-Transfer Radical Polymerization. *Angew. Chem., Int. Ed.* **2013**, *52*, 9125–9129.
56. Dunderdale, G. J.; Urata, C.; Miranda, D. F.; Hozumi, A. Large-Scale and Environmentally Friendly Synthesis of pH-Responsive Oil-Repellent Polymer Brush Surfaces under Ambient Conditions. *ACS Appl. Mater. Interfaces* **2014**, *6*, 11864–11868.
57. Shah, R. R.; Merreceyes, D.; Husemann, M.; Rees, I.; Abbott, N. L.; Hawker, C. J.; Hedrick, J. L. Using Atom Transfer Radical Polymerization To Amplify Monolayers of Initiators Patterned by Microcontact Printing into Polymer Brushes for Pattern Transfer. *Macromolecules* **2000**, *33*, 597–605.
58. Liu, X.; Dai, B.; Zhou, L.; Sun, J. Exponential Growth of Layer-by-Layer Assembled Coatings with Well-Dispersed Ultrafine Nanofillers: a Facile Route to Scratch-Resistant and Transparent Hybrid Coatings. *J. Mater. Chem.* **2009**, *19*, 497–504.